Mater. Res. Soc. Symp. Proc. Vol. 1774 © 2015 Materials Research Society
DOI: 10.1557/opl.2015.706

Investigation of Thermoelectric Properties of *P*-Type GaN Thin Films

Bahadir Kucukgok[1], Babar Hussain[1], Chuanle Zhou[1], Ian T. Ferguson[2], Na Lu[3]

[1]Department of Electrical and Computer Engineering, University of North Carolina at Charlotte, 9201 University City Blvd, Charlotte, NC 28223, U.S.A
[2]College of Engineering and Computing, Missouri University of Science and Technology, 305 McNutt Hall, 1400 N. Bishop, Rolla, MO 65409, U.S.A
[3]Department of Engineering Technology, University of North Carolina at Charlotte, 9201 University City Blvd, Charlotte, NC 28223, U.S.A

ABSTRACT

GaN and its alloys are promising candidates for high temperature thermoelectric (TE) materials due to their high Seebeck coefficient and high thermal and mechanical stability. Moreover, these materials can overcome the toxicity concern of current Te-based TE materials, such as Bi_2Te_3 and PbTe. These materials have recently shown a higher Seebeck coefficient than that of SiGe in high temperature region because their large bandgap characteristic eliminates the bipolar conduction. In this study, we report the room temperature thermoelectric properties of p-type Mg doped GaN, grown by metalorganic chemical vapor deposition (MOCVD) on sapphire substrate with various carrier concentrations. Undoped and n-type GaN are also incorporated with p-type GaN films to make comparison. The structural, optical, electrical, and thermal properties of the samples were examined by X-ray diffraction, photoluminescence, van der Pauw hall-effect, and thermal gradient methods, respectively. The Seebeck coefficient ranging from 710-900μV/K at room temperature of Mg: GaN were observed, which further indicated their potential TE applications.

INTRODUCTION

High-temperature thermoelectric (TE) materials have attracted significant attention in recent decades for researches due to the increasing demand for alternative energy technology [1-6]. Owing to Seebeck effect, waste heat can be directly converted into electricity by using TE devices in which they can generate electricity from temperature difference and vice versa [1,5,7-9]. Therefore, consumption of current energy resources such as, fossil fuels could be eliminated with implementing TE conversion technology [10-12]. Additionally, TE devices have several advantages over other power sources, such as long life time, no moving parts, non-toxicity, and high reliability, which makes them widely used in various areas including space applications, automotive, on-chip cooling, and recently for solar-thermal electrical-energy generation [2,4,13].

The quality of a TE material is related to dimensionless figure of merit, namely ZT, and expressed as $ZT=(S^2\sigma)/\kappa$ where S, σ, T, and κ are the Seebeck coefficient, electrical conductivity, absolute temperature, and thermal conductivity, normally the sum of electronic and lattice contributions, $\kappa=\kappa_e+\kappa_l$, respectively [2,8,12-14]. For enhanced value of ZT for a TE material; a large value of Seebeck coefficient, high electrical conductivity, and a low thermal conductivity are necessary [5,10,15]. In other words, maximized power factor ($S^2\sigma$) and/or minimized total thermal conductivity ($\kappa_e+\kappa_l$) need to be achieved. However, this is a difficult task because electrical and thermal properties are interdependent with each other [8,10]. For that reason, it is

still one of the major drawbacks to individually tune these properties, and numerous approaches have been performed toward improving the *ZT* [7,16]. Most commonly ones are to reduce the lattice thermal conductivity by introducing host atoms with different atomic mass and creating phonon scattering centers in the structure to deteriorate the mean free path of heat carrying phonons through alloying and nanostructuring, respectively [4,9]. Additionally, power factor enhancement via engineering the bandstructure through tuning the resonant impurity levels near the Fermi level, and band convergence/degeneracy results in high *ZT* values [3].

Currently TE materials research mainly focuses on Bi_2Te_3 and PbTe based, and SiGe. However, these materials are rare, toxic, expensive raw materials, and unstable at elevated temperatures [2,5,11]. Therefore, recent efforts have been conducted to find new TE materials with modified structural and composition to reduce lattice thermal conductivity and increase Seebeck coefficient due to the electrons confinement [1,2,4]. Furthermore, wide bandgap semiconductors such as, III-nitrides [6,12] have been studied as new TE materials and substantial improvement on *ZT* have lately been achieved because of their enhanced electrical conductivity via doping without affecting the thermal conductivity too much at the same time.

In particular, considering high carrier density ($\geq 10^{19} cm^{-3}$) p-type materials, power factor ($S^2\sigma$) can be improved owing to their sophisticated valance band structure, which has various pockets in the Fermi surface [14] as well as high impurity scattering, which results in low lattice thermal conductivity. For instance, *ZT* values of 2.4 at 300K and 3 at 550K were achieved by using p-type Bi_2Te_3/Sb_2Te_3 superlattice and PbSeTe/PbTe quantum dot, respectively [8]. Achieving p-type doping in GaN becomes a major issue due to Mg acceptor's high activation energies of 100-200meV [17]. Acceptor dopants such as Mg, Be, C, and Zn have been used for p-type doping but Mg is the most common and often used among them. To enhance p-type conductivity in GaN, codoping with oxygen and hydrogen has also been studied to increase the solubility and compensate the unintentional defects that caused n-type conductivity.

In the present study, we studied room temperature TE properties of Mg doped GaN, grown by metalorganic chemical vapor deposition (MOCVD) on sapphire substrate with various carrier concentrations. Undoped and n-type GaN are also incorporated with p-type GaN films to make comparison. The structural, optical, electrical, and thermal properties of the samples were examined by X-ray diffraction, photoluminescence, van der Pauw hall-effect, and thermal gradient methods, respectively.

EXPERIMENT

The samples studied here include thin films p-type, undoped, and n-type GaN. GaN thin film samples were grown on c-axis 2 in. sapphire wafer by metal organic vapor deposition method (MOCVD) with various doping concentrations. P-type GaN was achieved using Mg as an acceptor dopant. The standard in-plane Seebeck measurement is performed in this study. Details of the theory and experiments setup were discussed in elsewhere [18]. The electrical characterizations were performed by hall effect measurement methods in the in-plane direction. For Seebeck and hall measurements, Ni/Au ohmic electrodes were deposited on the top p-GaN layers followed by thermal annealing at 650°C for about 8 minutes under nitrogen ambient. Moreover, high resolution x-ray diffraction (HRXRD) measurements were performed using a Philips X'Pert MRD triple-axis diffractometer equipped with a four crystals Ge (220) monochromator in the incident beam optics and a Cu sealed anode and room temperature

photoluminescence (PL) analyses by utilizing deep ultraviolet (DUV) spectroscopy (excitation at 248nm), to investigate the effect of structural and optical properties of the samples, respectively.

DISCUSSION

The dependence of electrical conductivity (σ) and mobility (μ) on carrier density at 300K is shown in Figures 1 (a) and (b), respectively. Carrier densities were measured as $8.34\times10^{16}cm^{-3}$, $2.12\times10^{17}cm^{-3}$, $3.19\times10^{17}cm^{-3}$, and $4.05\times10^{17}cm^{-3}$. Both hall measurement and temperature gradient Seebeck measurements confirm that samples are p-type. Trends of increasing electrical conductivity and decreasing mobility with increasing carrier density were observed. The electrical conductivity and mobility of p-type samples are much lower compare to that of n-type GaN ($\sigma\geq90\Omega^{-1}cm^{-1}$ and $\mu\geq390cm^{2}V^{-1}s^{-1}$). This is because high impurity concentration induces defects which result in introducing more scattering centers in the film hence causes low electrical conductivity and hole mobility. Figure 2 illustrates the rocking curve HRXRD of p-type GaN sample and reveals that introducing Mg into the lattice matrix degenerate the crystal quality with having broader full width at half maximum (FWHM) 374arcsec and higher screw dislocation density $1.43\times10^{8}cm^{-2}$. The other reason of low electrical conductivity of p-type GaN samples is because Mg, as an acceptor dopant, has low solubility [19] and high ionization energy (~200meV). Additionally, existence of high background electron concentration is the other main hindrance for having high p-type conductivity.

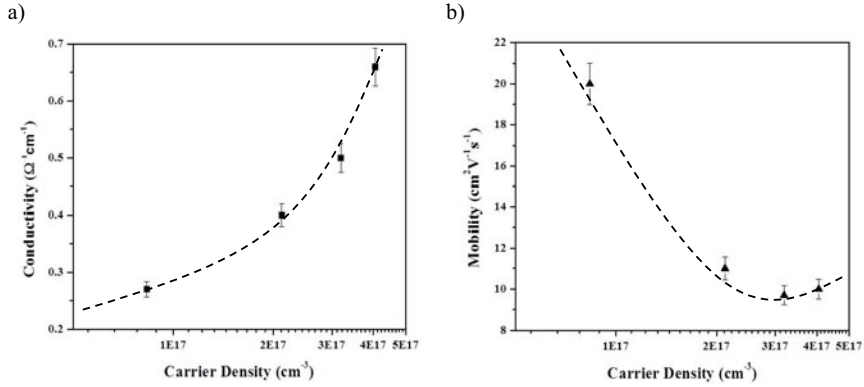

Figure 1: (a) Electrical conductivity and (b) mobility of Mg doped GaN thin films at 300K as a function of carrier density. Dashed lines are guided to the eye.

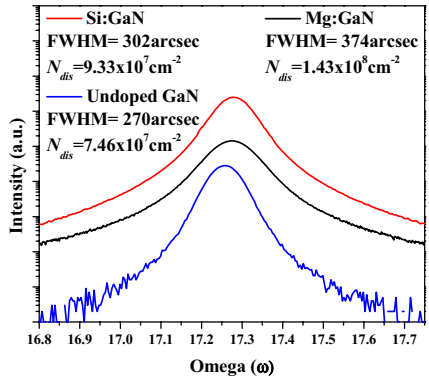

Figure 2: HRXRD rocking curve analysis of p-type GaN compared with n-type GaN. FWHM and screw and mixed dislocation densities (N_{dis}) are included as well for comparison.

The Seebeck and power factor results of the Mg doped GaN presented in Figures 3 (a) and (b), respectively.

a)

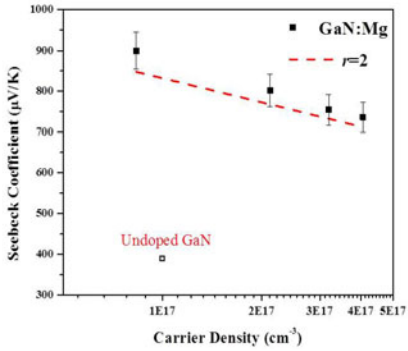

b)

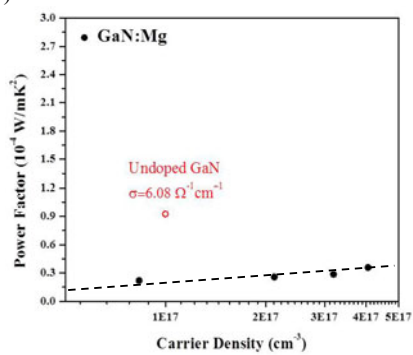

Figure 3: (a) Seebeck coefficient and (b) power factor of Mg doped thin film GaN with varying carrier densities at 300K (Dashed line is guided to the eye). In Figure 3 (a), the dash linear fit line (r=2, acoustical phonon scattering) is generated by using equation 1 in order to make comparison of theoretical and experimental values of Seebeck.

Increasing the electrical conductivity, which is a function of the doping concentration, without experiencing much deterioration in the Seebeck coefficient, could increase the power factor as observed in Figure 3 (b). Seebeck coefficient can be expressed with Mott-Jones relation to simple transport models [20] and defined as

$$S = \frac{k_B}{e}\left(r + \frac{5}{2} + \ln\left(\frac{2(2\pi m^* kT/h^3)^{3/2}}{n}\right)\right) \quad (1)$$

where n, r, k, m^*, and h are the carrier density, a factor related to scattering mechanism, Boltzmann constant, DOS effective mass, and Planck constant respectively. According to the equation 1, the electrical conductivity increases with doping level, and the Seebeck coefficient decreases as illustrated in Figure 3 (a). P-type GaN materials typically have higher Seebeck coefficients than n-type materials and our Mg doped GaN samples exhibited a much higher Seebeck coefficient than n-type GaN (Figure 3 (a)). The calculated Seebeck coefficient with varying carrier density shown as red dash line is also integrated in Figure 3 (a) to estimate the major scattering factor as well as show the measured and calculated Seebeck coefficients are in agreement. The acoustical phonon scattering (r=2) at 300K using density of states (DOS) effective mass of m_d*=1.1m_h; which is a most common literature value taken for p-type wurtzite GaN, are considered for equation 1. The significant Seebeck coefficient difference between p-type GaN and n-type GaN at similar carrier densities can be attributed to their effective mass variation while carrier density increases (equation 1).

The power factor of n-type GaN was much higher than that of p-type GaN as illustrated in Figure 3 (b); although p-type GaN samples demonstrated the highest Seebeck coefficients (Figure 3 (a)). It is due to the very low electrical conductivity of Mg doped GaN and it is a clear evidence of the inverse relationship between electrical conductivity and the Seebeck coefficient, which has been shown in other materials.

PL measurements are performed on p-type GaN samples at 300K and realized that there is a correlation between Seebeck coefficient and power factor. As the bandgap is decreasing the Seebeck and power factors are increasing except of the sample 4 (Table 1); however, in order to understand the underneath mechanism, more detail study needs to performed. The measurement results of TE, electrical, and PL characterizations are summarized in Table 1.

Table 1: Seebeck coefficient, power factor, electrical conductivity, mobility, carrier density, and energy bandgap of Mg doped GaN.

Material	Seebeck Coefficient (μV/K)	Power Factor (10^{-4}W/mK^2)	Conductivity (Ω^{-1}cm^{-1})	Mobility (cm^{2}V^{-1}s^{-1})	Carrier Density (cm^{-3})	Energy Bandgap (eV)
GaN:Mg	900	0.21	0.27	20	8.34×10^{16}	3.39
GaN:Mg	802	0.25	0.40	11	2.12×10^{17}	2.90
GaN:Mg	754	0.28	0.50	9.7	3.19×10^{17}	2.89
GaN:Mg	736	0.35	0.66	10	4.05×10^{17}	3.39

CONCLUSIONS

Mg doped p-type GaN thin films are studied by examining their electrical and thermal properties. It was found that Seebeck coefficient of p-type GaN is much higher than that of n-type ones, however their power factor is considerably lower compared to n-type GaN. The high Seebeck coefficient does not compensate the low electrical conductivity of p-type doping. In this study, the Highest Seebeck coefficient 900μV/K and power factor 0.35×10^{-4}W/mK^2 of p-type GaN are observed at 8.34×10^{16}cm^{-3} and 4.05×10^{17}cm^{-3}, respectively. The significant variance of

Seebeck values between p-type and n-type GaN could be attributed to their different effective masses, which has dominant role on DOS and thus Seebeck coefficient.

REFERENCES

1. C.-G. Han, B.-P. Zhang, Z.-H. Ge, L.-J. Zhang, Y.-C. Liu, *J Mater Sci.* **48**, 4081–4087 (2013).
2. D. Li, R.-R. Sun, X.-Y. Qin, *Progress in Natural Science: Materials International*, **21**, 336−340 (2011).
3. G. Tan, L.-D. Zhao, F. Shi, J. W. Doak, S.-H. Lo, H. Sun, C. Wolverton, V. P. Dravid, C. Uher, and M. G. Kanatzidis, *J. Am. Chem. Soc.* **136**, 7006−7017 (2014).
4. L. Xu, Y. Liu, B. Chen, C. Zhao, K. Lu, *Polym. Compos.* **34**, (2013).
5. Z. Chen, Y.M. Han, M. Zhou, C.M. Song, R.J. Huang, Y. Zhou, and L.F. Li, *Journal of Electronic Materials*, **43** (2014).
6. E. N. Hurwitz, B. Kucukgok, A. G. Melton, Z.Q. Liu, N. Lu, and I. T. Ferguson, *MRS Proceedings*, **1396** (2012).
7. C.Xiao, K. Li, J. Zhang, W. Tong, Y. Liu, Z. Li, P. Huang, B. Pan, H. Sud, and Y. Xie, *Mater. Horiz.* **1**, 81−86 (2014).
8. O. C. Yelgel and G. P. Srivastava, *J. Appl. Phys.* **113**, 073709 (2013).
9. R. J. Korkosz, T. C. Chasapis, S.-H. Lo, J. W. Doak, Y. J. Kim, C.-I. Wu, E. Hatzikraniotis, T. P. Hogan, D. N. Seidman, C. Wolverton, V. P. Dravid, and M. G. Kanatzidis, *J. Am. Chem. Soc.* **136**, 3225−3237 (2014).
10. B. Du, Y. Saiga, K. Kajisa, and T. Takabatake, *Chem. Mater.* **27**, 1830−1836 (2015).
11. M. Jost, J. Lingner, M. Letz, and G. Jakob, *Semicond. Sci. Technol.* **29**, 124011 (2014).
12. N. Lu and I. Ferguson, *Semicond. Sci. Technol.* **28**, 074023 (2013).
13. K. P. Ong, D. J. Singh, and P. Wu, *Physical Review B*, **83**, 115110 (2011).
14. C. M. Jaworski, M. D. Nielsen, H. Wang, S. N. Girard, W. Cai, W. D. Porter, M. G. Kanatzidis, and J. P. Heremans, *Physical Review B*, **87**, 045203 (2013).
15. J.-I. Tani and H. Kido, *Jpn. J. Appl. Phys.* **46**, (2007).
16. J. P. Heremans, B. Wiendlochaac, and A. M. Chamoire, *Energy Environ. Sci.* **5**, 5510 (2012).
17. A. Nakajima, P. Liu, M. Ogura, T. Makino, S.-I. Nishizawa, S. Yamasaki, H. Ohashi, K. Kakushima, and H. Iwa, *Appl. Phys. Express*, **6** ,091002 (2013).
18. B. Kucukgok, B. Wang, A. G. Melton, N. Lu, and I. T. Ferguson, *Phys. Status Solidi C*, **11,** 894–897 (2014).
19. C. G. V. D. Walle, *SPIE* **3283**, (1998).
20. S. Yamaguchi, Y. Iwamura, A. Yamamoto, *Appl. Phys. Lett*. **82**, (2003).